

# ACCOUNTS of CHEMICAL RESEARCH®

OCTOBER 2005

*Registered in U.S. Patent and Trademark Office; Copyright 2005 by the American Chemical Society*

## ARTICLES

### Confinement of Metal Complexes within Porous Hosts: Development of Functional Materials for Gas Binding and Catalysis

LEILANI L. WELBES AND A. S. BOROVIK\*  
*Department of Chemistry, University of Kansas, 2010 Malott Hall, 1251 Wescoe Drive, Lawrence, Kansas 66045*

#### ABSTRACT

The development of porous functional materials, using template copolymerization, that function in gas binding/release and catalysis is described. Using substitutionally inert metal complexes as templates, materials were prepared with immobilized sites that retained structural properties of the template; this allows for tunable functional properties. Chemical modification of the immobilized sites led to coordinatively unsaturated metal centers that reversibly bind either O<sub>2</sub> or NO. Materials have also been prepared that exhibit varying degrees of catalytic activity in the hydrolytic kinetic resolution of epoxides as a function of the template concentration used to prepare the polymers.

#### Introduction

Progress in the design and synthesis of metal complexes has led to the preparation of molecular systems that have varying degrees of control over the primary and secondary coordination spheres around the metal ions.<sup>1</sup> Synchroni-

Leilani L. Welbes (born in 1976) was raised in Tomahawk, WI, and obtained her B.S. in chemistry (1999) from the University of Wisconsin—River Falls. She attended the University of Kansas for her Ph.D. in chemistry (2005), working with A. S. Borovik on the development of porous solids that function as heterogeneous catalysts. She is currently a postdoctoral associate at the University of Michigan with Professor Melanie Sanford.

A. S. Borovik is a professor of chemistry at the University of Kansas. His biography appeared recently in an Account on the utility of hydrogen bonds in synthetic metal complexes.<sup>1</sup>

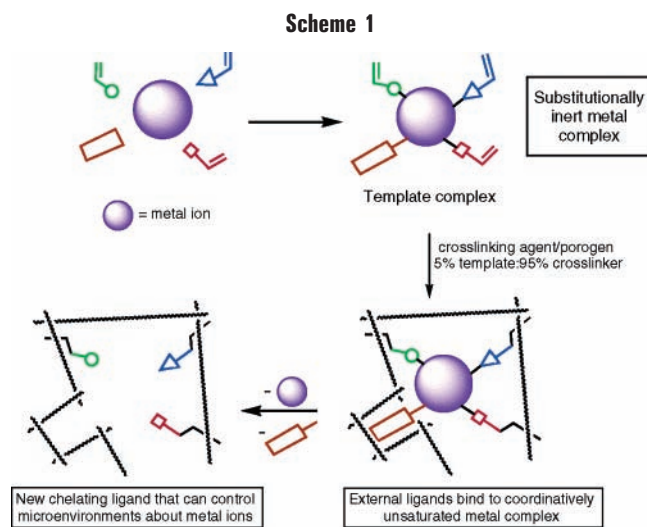
zation of the coordination spheres allows for the regulation of functional properties such as Lewis acidity, redox processes, and selectivity. Systems with these tunable properties are commonly molecular species having length scales on the order of 1–5 nm. Extending these structure/function relationships to systems of larger lengths, such as polymers, is often difficult because of complexities associated with positioning key structural components around the metal ion(s). Therefore, one current challenge is to prepare functional materials having the same level of structural control around reactive metal sites as found in their low molecular weight analogues.

Our approach toward solving this problem is to confine metal complexes within porous organic frameworks. We have utilized template copolymerization, a method used to prepare molecularly imprinted polymers,<sup>2,3,4</sup> to prepare functional porous materials derived from metal-based molecular precursors.<sup>5,6</sup> This strategy is advantageous because it potentially allows for structural control over the coordination spheres of metal complexes after immobilization into a porous host. This Account describes our recent efforts in developing materials that exhibit function in the storage and release of dioxygen<sup>5a,b</sup> and nitric oxide<sup>5c,d</sup> and in catalysis.<sup>6</sup>

#### General Methodology

Scheme 1 outlines the general copolymerization process used to prepare our porous materials.<sup>5,6</sup> This methodology in principle allows for partial control of the size and shape of the immobilized sites within a network polymer. We reasoned that this method could be applied to the design and preparation of new multidentate ligands dispersed throughout a porous material. Because their molecular structures are fixed prior to copolymerization, substitutionally inert metal complexes serve as templates to produce immobilized sites with uniform architecture. In addition, by varying the concentration of the immobilized

\* To whom correspondence should be addressed. Telephone: 785-864-4067. Fax: 785-864-5396. E-mail: aborovik@ku.edu.



template, the secondary coordination sphere of the immobilized metal complexes can be further modulated. The regulation of structure within the immobilized sites should allow for the development of materials for various applications.

This copolymerization methodology yields highly cross-linked and porous solids as depicted schematically in Figure 1. Although the hosts are amorphous, the immobilized site structures are sufficiently defined to allow for controlled function and have high accessibility via the porous network. This approach differs from many other methods of metal complex immobilization, which emphasize attachment of metal complexes to preformed supports. For instance, chemical modification of linear and slightly cross-linked (2–20%) supports<sup>7,8</sup> usually limits attachment of complexes to the polymer surface. In addition, the resulting materials are often flexible polymers, because of the low degree of cross-linking, which limits the control over the environment around the metal ion(s). Another common method involves the encapsulation of metal complexes within preformed porous networks, such as zeolites.<sup>9</sup> However, these systems limit the ability to fine tune the environment around the metal



**FIGURE 1.** Schematic illustrating a porous solid containing immobilized metal complexes. Blue spheres represent the metal ions, and the hash lines symbolize the porous amorphous host.

complex, and attachment often occurs through noncovalent interactions that can lead to the loss of metal.<sup>10</sup>

Our approach to prepare materials is aligned with molecular approaches, such as those used by Lehn,<sup>11</sup> Yaghi,<sup>12</sup> and Long<sup>13</sup> in which porous systems in the crystalline phase have been prepared from metal complexes. Many of these systems have led to materials that exhibit new physical properties,<sup>12,13</sup> while others are potentially useful in catalysis, sensor development, and ion recognition.<sup>11,12</sup> In addition, the imprinted dendrimers of Zimmerman regulate structure by incorporating elements of polymer imprinting into molecular species.<sup>14</sup> We, too, use molecular precursors as building blocks for porous materials.<sup>5,6</sup> Copolymerization of the inert metal templates with excess cross-linker results in materials that are sufficiently rigid, allowing for retention of the immobilized site and pore structure generated during polymerization. The porosity of the host allows substrate and solvent access to the immobilized sites within the material. Covalent linkage of complexes to the host limits leaching of the complexes. Moreover, tuning variables such as template structure and concentration of the template immobilized within the polymer serve to modulate the function of the materials.

## Probing Site Structure

Little is known about the structure of the immobilized sites in many of the materials prepared by template copolymerization because most systems incorporate organic-based templates.<sup>15</sup> Traditional spectroscopic techniques used for analysis of organic compounds have difficulty distinguishing the immobilized site structure from the host, which is present in large excess compared to the organic template, making site structure determination problematic. Structures of immobilized sites are thus usually inferred through rebinding studies.<sup>16</sup> Using inorganic templates, we take advantage of the inherent properties of metal complexes and can utilize spectroscopic methods that are selective for metal ions, such as X-ray absorption (XAS) and electron paramagnetic resonance (EPR) spectroscopies.<sup>5,6,17</sup>

Using this approach, we developed an endogenous ligand-binding assay involving unsaturated  $\text{Co}^{\text{II}}$  complexes to analyze immobilized site structure.<sup>5a,b</sup> This assay uses square planar  $[\text{Co}^{\text{II}}\text{salen}]$  complexes (salen, bis[2-hydroxybenzaldehyde]ethylene-diimine), which are known in solution to weakly bind a fifth ligand (e.g.,  $\text{O}_2$  or pyridine) with association constants of less than  $100 \text{ M}^{-1}$ .<sup>18</sup> However, five-coordinate  $[\text{Co}^{\text{II}}\text{salen}(\text{py})]$  complexes with square pyramidal geometry exhibit a strong affinity for dioxygen ( $K_a > 10^4 \text{ M}^{-1}$ ) and readily form the six-coordinate  $[\text{Co}\text{salen}(\text{py})(\text{O}_2)]$  species.  $[\text{Cosalen}]$ ,  $[\text{Cosalen}(\text{py})]$ , and  $[\text{Cosalen}(\text{py})(\text{O}_2)]$  have distinct EPR properties, making it possible to probe the structural and functional properties of the immobilized complexes within porous materials.

Figure 2 depicts schematically the design concepts for this system. A substitutionally inert, six-coordinate  $\text{Co}^{\text{III}}$  complex is immobilized within the material to create sites having similar structure and to ensure that ligand placement around the metal ion is maintained during the

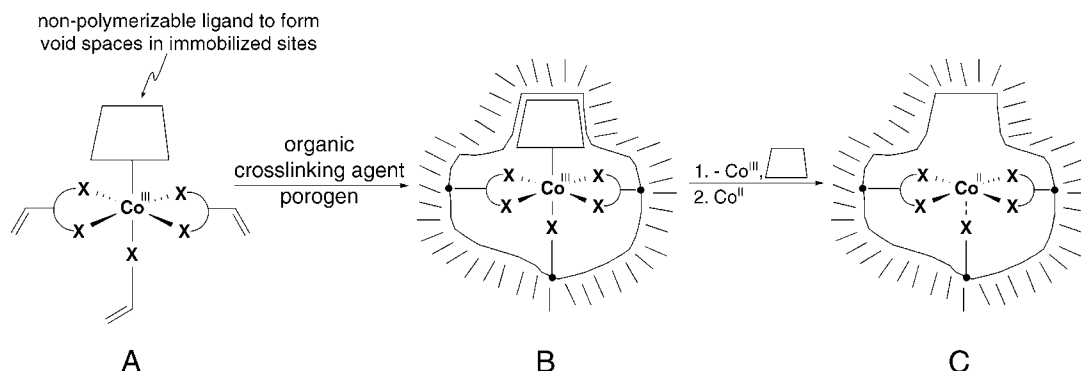


**FIGURE 2.** Schematic illustrating the template copolymerization method used for preparing coordinatively unsaturated metal sites immobilized within porous materials. Shown are the substitutionally inert  $\text{Co}^{\text{III}}$  complex used to form the immobilized sites after copolymerization (B), and chemically modified immobilized sites containing coordinatively unsaturated  $\text{Co}^{\text{II}}$  complexes (C).

polymerization process (Figure 2A). Immobilization of the template occurs through three points of attachment to the porous host, with two being from the salen ligand and one from an axially bound ligand. The other axial position is filled by a ligand without polymerizable functional groups, of which the only connection to the polymer is through the  $\text{Co}^{\text{III}}$  center (Figure 2B). This remaining ligand can be removed postpolymerization to create space for the rebinding of other external ligands. Chemical modification of the active sites after polymerization results in removal of the cobalt ion and nonpolymerizable ligand. Rebinding of  $\text{Co}^{\text{II}}$  ions produces coordinatively unsaturated four-coordinate  $\text{Co}^{\text{II}}$  sites with an endogenous ligand installed within the sites (Figure 2C).

The porous polymer used in this study was  $\text{P-1}\cdot\text{py}[\text{Co}^{\text{II}}]$ , for which the preparation is shown in Scheme 2.<sup>5b</sup> The template used was  $[\text{Co}^{\text{III}}(\text{vpy})(\text{dmap})]\text{PF}_6$ , where the salen ligand is modified with two styryloxy groups in the 4-positions. A 4-vinyl-pyridine ligand serves as one of the axial ligands, and the remaining coordination site is occupied by a 4-(dimethylamino)pyridine (dmap) ligand. After copolymerization is complete, the salen and vinyl pyridine ligands are covalently connected to the porous poly(methacrylate) host, with the axially pyridine installed perpendicular to the cobalt salen plane. Reduction of  $\text{Co}^{\text{III}}$  to  $\text{Co}^{\text{II}}$  allows for removal of the cobalt ion and dmap ligand from the immobilized sites to afford apo polymer,  $\text{P-1}\cdot\text{py}$ ; 90% of the immobilized sites rebind  $\text{Co}^{\text{II}}$  after treatment with  $\text{Co}(\text{OAc})$ .

We were initially interested in the position of the endogenous axial pyridine relative to the  $\text{Co}^{\text{II}}$  salen complex.<sup>5b</sup> There are two general possibilities: (1) the structure of the immobilized sites is rigid, resulting in a predominance of five-coordinate sites because the  $\text{Co}^{\text{III}}$  template complex predisposes the pyridine ligand to bind the cobalt center, and (2) the structure of the immobilized sites is relatively flexible, yielding a distribution of four- and five-coordinate cobalt sites within the material, similar to what is observed for monomeric analogues in solution.<sup>18</sup> X-band EPR results obtained for  $\text{P-1}\cdot\text{py}[\text{Co}^{\text{II}}]$  suspended in various solvents show that the material contains a mixture of immobilized sites composed of four- and five-coordinate complexes, with results consistent with possibility 2.<sup>5b</sup> The greatest number of five-coordinate immobilized sites ( $\sim 60\%$ ) is observed when the polymer is

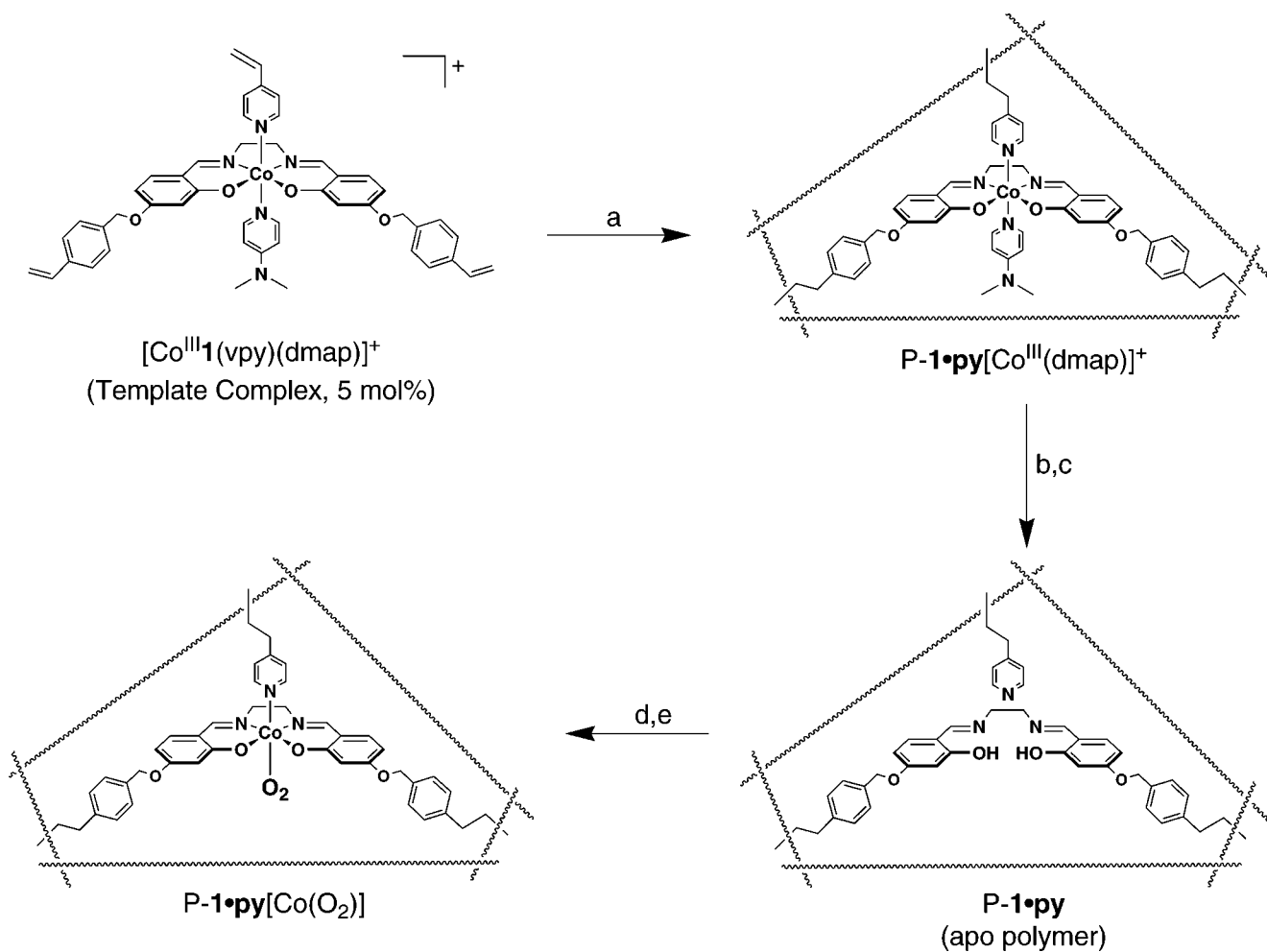
suspended in the same solvent ( $\text{CH}_3\text{NO}_2$ ) used to prepare the material. Conversely, the ratio of five- to four-coordinate sites decreased for materials suspended in other solvents, such as cyclohexane and ether, which have a different structure from that of the polymerization solvent.

### Immobilized Site Architecture

The picture that emerges from these studies is one in which an equilibrium exists between the four- and five-coordinate sites suggesting that ligands and complexes in the immobilized sites are more flexible than often depicted schematically (e.g., Scheme 1). On the basis of X-band EPR studies, it appears that the ligands within the sites are correctly positioned for the formation of five-coordinate complexes (Figure 3).<sup>5b</sup> However, in  $\text{P-1}\cdot\text{py}[\text{Co}^{\text{II}}]$ , there is enough flexibility within the immobilized sites so that the axial pyridine binds weakly to the  $\text{Co}^{\text{II}}$  center, similar to what is observed in solution for  $[\text{Co}^{\text{II}}\text{salen}]$ .<sup>18</sup>

We proposed that rotation of the bonds linking the template assembly to the host creates a somewhat dynamic immobilized site structure resulting in the distribution of four- and five-coordinate sites.<sup>5b</sup> This explanation highlights the importance of how a template is attached to the polymeric host. The three-point binding that was used to form the immobilized sites in  $\text{P-1}\cdot\text{py}[\text{Co}^{\text{II}}]$  is sufficient for covalent linkage of the template to the porous host and sustains the relative spatial orientation of the endogenous pyridine to the cobalt center. However, this number of linkages is not sufficient to rigidly maintain the thermodynamically unfavorable five-coordinate  $\text{Co}^{\text{II}}$  sites.

The findings with  $\text{P-1}\cdot\text{py}[\text{Co}^{\text{II}}]$  also show that the solvent used for polymer suspension plays a role in the distribution between four- and five-coordinate sites. Polymers suspended in the solvent used to grow the materials exhibited the highest percentage of five-coordinate sites, while this percentage decreased when the polymer was suspended in other noncoordinating solvents. We have proposed that a solvent memory effect within the sites affects the coordination geometry of the  $\text{Co}^{\text{II}}$  ions as a result of solvation of the template during copolymerization.<sup>5b</sup> Suspension of the polymer in the solvent used to grow the material (i.e.,  $\text{CH}_3\text{NO}_2$ ) yields

Scheme 2<sup>a</sup>

<sup>a</sup> Conditions: (a) EGDMA (94 mol %), CH<sub>3</sub>NO<sub>2</sub>, Ar, 60 °C, 24 h; (b) Na<sub>2</sub>S<sub>2</sub>O<sub>4</sub>, MeOH, Ar, 2 h; (c) (NMe<sub>4</sub>)<sub>2</sub>EDTA, MeOH, Ar, 24 h; (d) Co(OAc)<sub>2</sub>, MeOH, Ar, 6 h; (e) O<sub>2</sub>, CH<sub>3</sub>NO<sub>2</sub>.

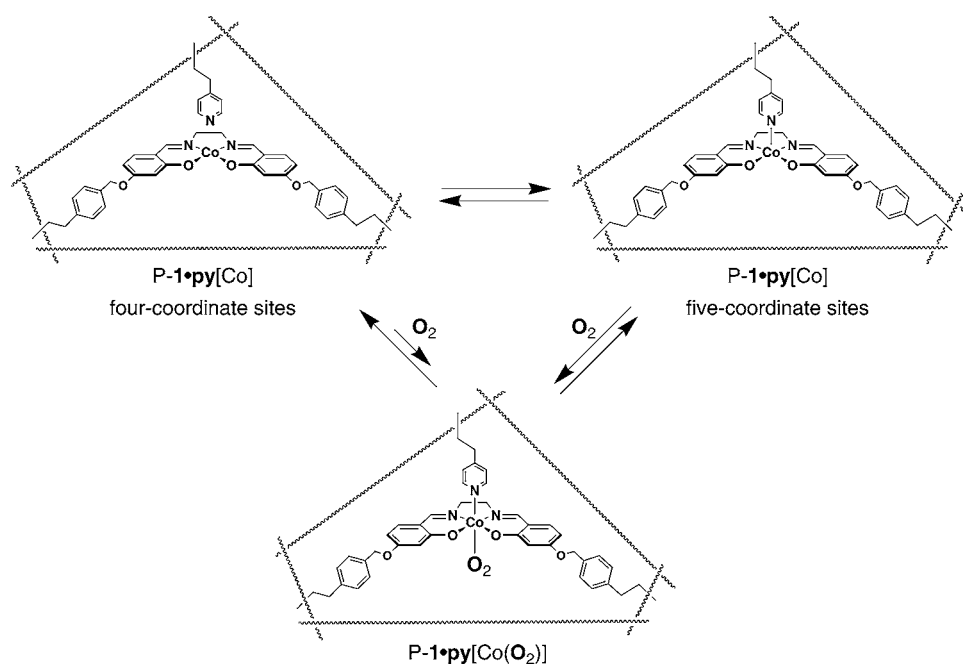


**FIGURE 3.** Schematic showing the proposed equilibria between immobilized four- and five-coordinate Co<sup>II</sup> sites in P-1•py[Co<sup>II</sup>].

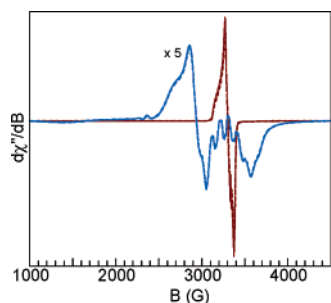


**FIGURE 4.** X-band EPR spectra measured at 77 K for nitromethane suspensions of P-1·py[Co<sup>II</sup>] (blue spectra) showing reversible dioxygen binding to form P-1·py[Co(O<sub>2</sub>)] (red spectra). Two cycles are presented: 1 (—) and 2 (- -).

immobilized sites with similar architecture to that originally templated; thus, the formation of five-coordinate complexes is favored. Suspension of the polymer in other solvents (e.g., ether and cyclohexane) gives rise to less organized sites, which leads to a higher percentage of the less ordered four-coordinate Co<sup>II</sup> complex. The solvent effect on endogenous ligand binding is similar to what is observed for exogenous species binding to other templated polymers. For example, the highest degree of a chiral template rebinding was observed in the solvent in which the polymer was prepared.<sup>19</sup>

### Functional Properties: Dioxygen Binding

Dioxygen binding to P-1·py[Co<sup>II</sup>] suggests that the endogenous pyridine ligands within the immobilized sites are within bonding distance of the cobalt centers (Figure 3).<sup>5b</sup> Exposure of a suspension of P-1·py[Co<sup>II</sup>] to dioxygen resulted in an EPR signal of a cobalt-dioxygen adduct. Spin concentration of the EPR signal indicated that up to 90% of the immobilized cobalt sites bound dioxygen. These results support the close spatial proximity of endogenous pyridine to the cobalt center within the immobilized sites, which is necessary for O<sub>2</sub> binding.<sup>19</sup> To corroborate this, a control polymer with four-coordinate Co<sup>II</sup> sites containing no endogenous pyridine ligands, P-1[Co<sup>II</sup>], was prepared and found to have minimal dioxygen binding (less than 5%).<sup>5a,b</sup>

The binding of dioxygen to P-1·py[Co<sup>II</sup>] is reversible. Purging suspended P-1·py[Co(O<sub>2</sub>)] with N<sub>2</sub> leads to the loss of the EPR signal for the cobalt-dioxygen adduct with concomitant appearance of the spectrum for P-1·py[Co<sup>II</sup>]. This sequence can be repeated several times without the apparent loss of the signal intensity for either P-1·py[Co<sup>II</sup>] or P-1·py[Co(O<sub>2</sub>)] (Figure 4). In solution, similar cobalt-dioxygen adducts dimerize to yield 1,2- $\mu$ -peroxo-bridged species,<sup>18,20</sup> formation of which is prevented in P-1·py[Co<sup>II</sup>] by the host.<sup>5a,b</sup> Our experiments with P-1·py[Co<sup>II</sup>] illustrate the site isolation capability of the host, which serves to stabilize the reactive cobalt-dioxygen adducts and allows reversible O<sub>2</sub> binding to occur.

### Functional Properties: Nitric Oxide Binding

The relationship of the nitric oxide (NO) concentration to biological effects ranging from protective to deleterious has spurred research into developing methods for the

storage and targeted release of NO.<sup>21,22</sup> We introduced porous materials containing immobilized metal nitrosyl complexes as one way to address this need.<sup>5c,d</sup> The initial system utilized immobilized four-coordinate [Co<sup>II</sup>salen] complexes within a porous host.<sup>5c</sup> This polymer was used as a control system in the dioxygen binding studies described above and has a low affinity for dioxygen.<sup>5a,b</sup> We anticipated that the immobilized Co<sup>II</sup> complexes should function as sites for NO binding<sup>5c</sup> based on the known efficient binding of NO to monomeric [Co<sup>II</sup>salen] in solution under anaerobic conditions.<sup>23</sup>

Exposure of P-1[Co<sup>II</sup>] to gaseous NO led to the formation of P-1[Co(NO)], which is marked by a noticeable color change of the material from orange to brown-green (Figure 5).<sup>5c</sup> XAS and EPR studies determined the storage and release properties of the material; heating the P-1[Co(NO)] at 120 °C under vacuum results in the release of NO to form P-1[Co<sup>II</sup>] over the course of 1 h. This process is reversible over several cycles. Under ambient pressure and temperature, the polymer exhibits a slower NO-release rate, with approximately 40% of the sites releasing NO over 14 days. The reversible NO binding found with P-1[Co<sup>II</sup>] contrast results reported for monomeric [Co<sup>II</sup>salen], which irreversibly binds NO in both solution and solid states.<sup>23</sup> We attribute this difference to the site isolation capability of the polymeric porous host.<sup>5c</sup> The host stabilizes the cobalt nitrosyl complex in [Co(salen)-(NO)] by isolation of the sites; this prevents bimolecular pathways leading to the formation of Co<sup>III</sup>-nitrite species [Co(salen)(NO<sub>2</sub>)], which is known to form under aerobic conditions.<sup>23</sup>

The results of gas uptake measurements shown in Figure 6 demonstrate the selective binding of NO by P-1[Co<sup>II</sup>] over other biologically relevant molecules such as CO<sub>2</sub>, O<sub>2</sub>, and CO.<sup>5c</sup> Exposure of solid samples of P-1[Co<sup>II</sup>] to 10.3 Torr of each gas resulted in 70% uptake of the NO available. Conversely, no apparent affinity of the immobilized cobalt sites for O<sub>2</sub>, CO, and CO<sub>2</sub> was detected. Control experiments were conducted with a polymer having no Co<sup>II</sup> ions coordinated to the immobilized salen sites, P-1, and a porous poly(EGDMA) polymer containing no immobilized sites to determine the importance of the Co<sup>II</sup> sites in NO absorption. Both control polymers demonstrated similar uptake values for each respective gas (~3  $\mu$ mol), establishing that minimal nonselective gas absorption had occurred and that the [Co<sup>II</sup>salen] sites were essential for selective NO binding.

### Functional Properties: Light-Activated NO Release

While P-1[Co<sup>II</sup>] selectively bound NO, it exhibited slow release of NO under ambient conditions.<sup>5c</sup> We sought to change the releasing properties of our material to allow for on-demand dispensing of NO through light initiation.<sup>5d</sup> Because the photolytic transfer of NO has been observed in solutions of monomeric [Ru(salen)(NO)] complexes,<sup>24</sup> we expected that a material containing immobilized [Ru(salen)(NO)] complexes would behave similarly.

The porous material P-1[Ru(NO)(Cl)], containing immobilized sites with bound nitric oxide (Figure 7), was

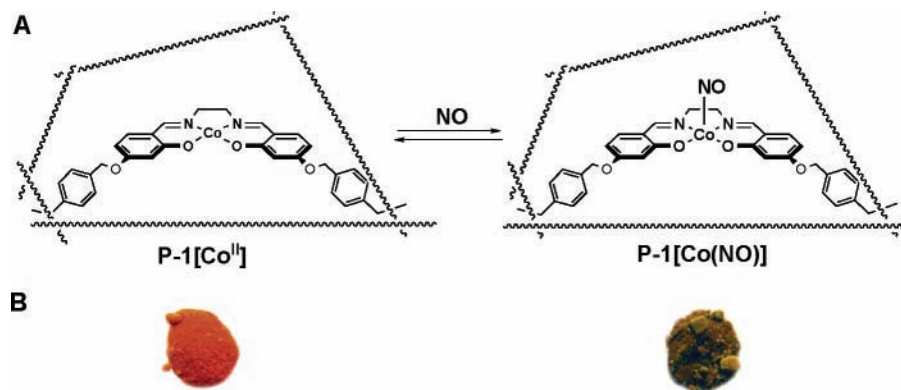


**FIGURE 5.** Schematic illustrating the reversible binding of NO observed in P-1[Co<sup>II</sup>] (A) and photographs of the color change observed in the materials upon NO binding (B).

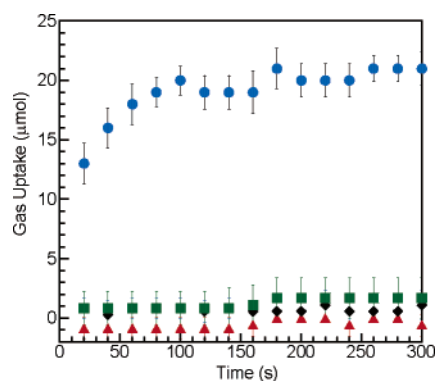


**FIGURE 6.** Gas binding versus time for P-1[Co<sup>II</sup>]. Legend of analyte gases: NO (●), O<sub>2</sub> (▲), CO<sub>2</sub> (■), and CO (◆).

prepared using similar synthetic procedures as outlined in Scheme 2, with [Ru<sup>I</sup>(NO)(Cl)] as a template.<sup>5d</sup> Analytical and spectroscopic studies indicate that the template retains its structure during copolymerization. X-band EPR spectroscopy was used to follow the photolytic release of NO from P-1[Ru(NO)(Cl)] as a result of broad-band irradiation with a Hg arc lamp. Photolysis of the material results in an X-band EPR spectrum in the solid state containing a rhombic signal with features at  $g = 2.3$ ,  $2.1$ , and  $1.8$ . These features are indicative of immobilized Ru<sup>III</sup> complexes that have lost NO with  $S = 1/2$  ground states,<sup>24c</sup> and the spectrum is indistinguishable from that of independently prepared P-1[Ru(Cl)]. The photolytic release of NO is also observed from suspensions of P-1[Ru(NO)(Cl)] in various solvents, with Figure 8 showing the absorbance spectrum obtained for a suspended sample in toluene irradiated at 370 nm.<sup>5d</sup> The characteristic absorbance features for P-1[Ru(Cl)] are observed at  $\lambda_{\text{max}} = 400$  (shoulder) and 660 nm.

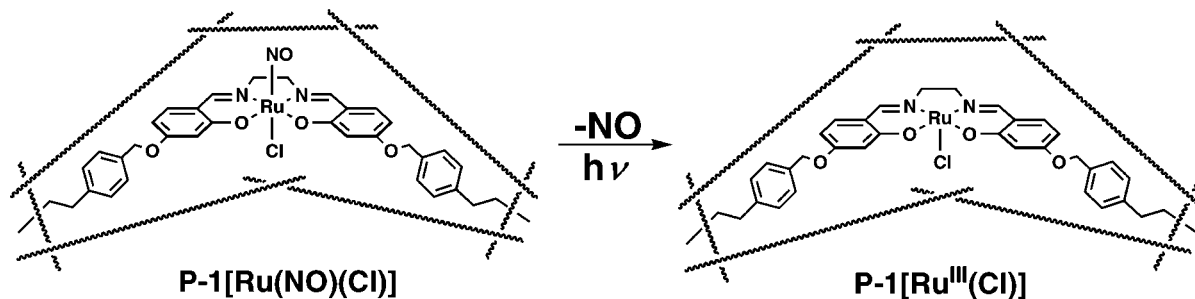
The amount of NO released from the material was determined indirectly using the Griess spectrophotometric method under physiological conditions.<sup>25</sup> A sample of P-1[Ru(NO)(Cl)] ranging in particle sizes from 0.5 to 1.0 mm irradiated for 80 min releases a maximum of 2.0 (4)  $\mu\text{mol}$  of NO/g of polymer as illustrated in Figure 9. Also shown in Figure 9 is a series of experiments demonstrating that NO release is only the result of sample irradiation. The sample was exposed to a series of light–dark–light sequences, and it was determined that NO release correlated to the irradiation stage of the sequences, while no

gas release was observed during the dark stage. These experiments are important because they show that the release of NO from P-1[Ru(NO)(Cl)] can be controlled with light under physiological conditions.

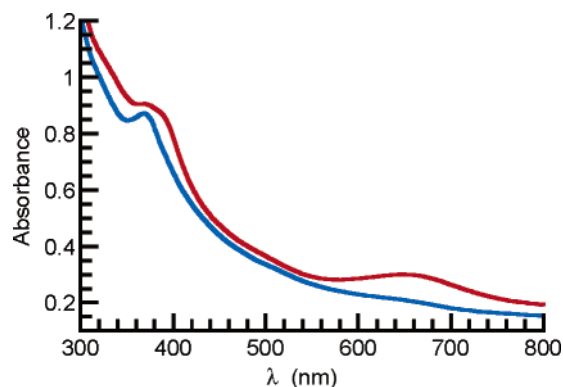
We have also demonstrated the transfer of NO from P-1[Ru(NO)(Cl)] to biomolecules such as equine skeletal muscle myoglobin (Mb).<sup>5d</sup> Figure 10 illustrates the transfer of NO from P-1[Ru(NO)(Cl)] to Mb under physiological conditions. Irradiation of P-1[Ru(NO)(Cl)] with 370 nm light resulted in 81% conversion of Mb to Mb(NO) over the course of 20 min. This transfer is shown in the absorption spectrum as a shift in the Mb Soret band from  $\lambda_{\text{max}} = 435$  to 420 nm, with similar properties observed in control spectra of equine skeletal muscle Mb and Mb(NO).

## Functional Properties: Catalysis

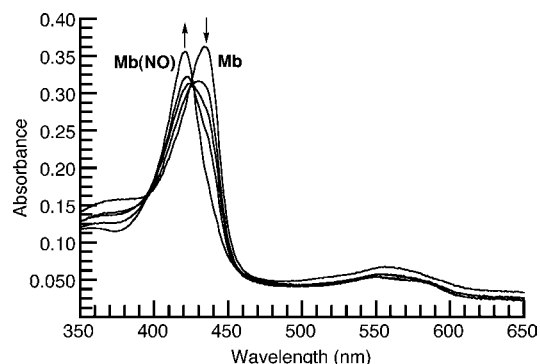
As part of our program to develop functional porous solids, we have also prepared materials that function as heterogeneous catalysts.<sup>6</sup> In the previously discussed materials used for gas binding, the immobilized sites were isolated from each other by the porous host. As a result, the function of reversible binding of O<sub>2</sub> and NO could be achieved by preventing bimolecular pathways that led to irreversible gas binding to monomeric species in solution. However, there are many transformations that require multiple metal complexes working together in concert to achieve function. We postulated that immobilized sites containing more than one metal center could be obtained by increasing the template/cross-linker ratio during copolymerization. This modification in the copolymerization process expands upon previous methodologies used to make site-isolated materials by allowing for the preparation of a wider array of porous polymers from a single template. *A priori*, if two metal centers are necessary for catalysis, then the resulting materials would display variable degrees of catalytic activity as a function of the template concentration. To test this proposal, a series of porous materials were prepared containing varying concentrations of a chiral cobalt-salen template to be used as heterogeneous catalysts in the hydrolytic kinetic resolution (HKR) of epoxides.<sup>26</sup> It has been proposed that in solution this reaction proceeds through a bimolecular pathway.<sup>26,27</sup> We thus anticipated that, as the concentra-



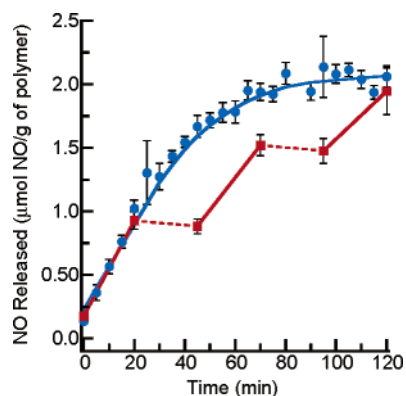
**FIGURE 7.** Materials containing immobilized Ru(NO) complexes that release NO upon irradiation with a broad-band Hg arc lamp.



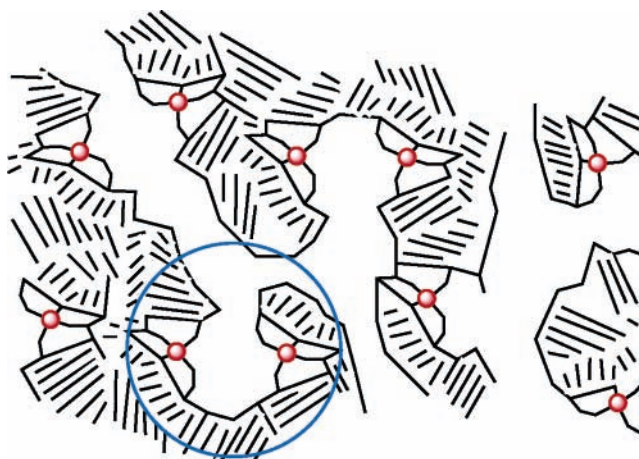
**FIGURE 8.** Absorbance spectra for P-1[Ru(NO)(Cl)] (blue) and P-1[Ru(III)(Cl)] (red) suspended in toluene.



**FIGURE 10.** Overlaid absorption spectra demonstrating the photolytic transfer of NO from P-1[Ru(NO)(Cl)] to  $3.0 \times 10^{-6}$  Mb in 50 mM phosphate buffer at pH 7.2.



**FIGURE 9.** Plot of NO release (in  $\mu\text{mol}$  of NO/g of polymer) as a function of time for particles between 0.5 and 1 mm. Continuous irradiation (●), light–dark–light sequences (■), irradiation phases (—), and dark phases (---).

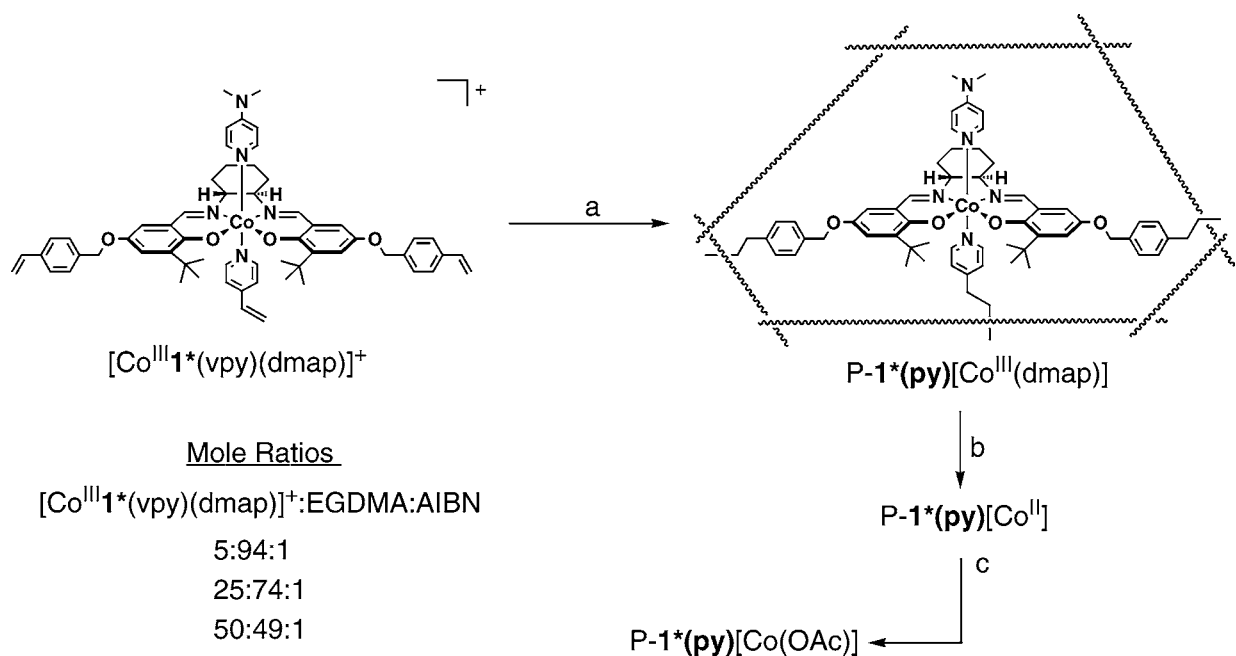


**FIGURE 11.** Schematic illustrating site–site interactions within a porous material.

tion of the template increases, more immobilized sites will be formed that have the correct orientation of cobalt complexes to promote catalytic activity (Figure 11).

Materials containing varying concentrations (5, 25, and 50 mol %) of immobilized sites derived from the template complex,  $[\text{Co}^{\text{III}}\text{I}^*(\text{vpy})(\text{dmap})]\text{PF}_6$ , were prepared according to the synthetic methods outlined in Scheme 3.<sup>6</sup> XAS and EPR spectroscopies were used to analyze materials containing 50 mol % template at all points in the synthetic process. XAS measurements are consistent with six-coordinate  $\text{Co}^{\text{III}}$  complexes immobilized within the porous host for the initial material formed, P-1\*(py)[ $\text{Co}^{\text{III}}(\text{dmap})$ ], indicating that the template maintains its structure during the polymerization process; these measurements are identical with results obtained for the monomeric tem-

plate complex,  $[\text{Co}^{\text{III}}\text{I}^*(\text{vpy})(\text{dmap})]^+$ . In addition, a comparison of the XANES spectrum for the reduced polymer, P-1\*(py)[ $\text{Co}^{\text{II}}$ ], with a reference polymer, P-1[ $\text{Co}^{\text{II}}$ ],<sup>17</sup> suggests that somewhat less than half of the cobalt sites have been reduced in P-1\*(py)[ $\text{Co}^{\text{II}}$ ].<sup>6</sup> X-band EPR data corroborate that a portion of the immobilized cobalt sites are reduced, having a square planar coordination geometry with a  $S = 1/2$  ground state.<sup>5a–c,28</sup> These results suggest that the endogenous pyridine ligand is not coordinated to most of the immobilized  $\text{Co}^{\text{II}}$  centers in P-1\*(py)[ $\text{Co}^{\text{II}}$ ], which is consistent with the known weak binding of pyridine to four-coordinate  $\text{Co}^{\text{II}}(\text{salen})$  complexes (*vide supra*).<sup>18</sup> The immobilized  $\text{Co}^{\text{II}}$  centers could be oxidized in the presence of acetic acid under aerobic conditions; oxidation is

Scheme 3<sup>a</sup>

<sup>a</sup> Conditions: (a) EGDMA, AIBN, DMF, 65 °C, Ar; (b) FeCp<sub>2</sub><sup>\*</sup>, CH<sub>2</sub>Cl<sub>2</sub>, Ar, rt; (c) HOAc, air, toluene, rt.

**Table 1. Hydrolytic Kinetic Resolution of Propylene Oxide Using Materials of Varying Template Concentration<sup>a</sup>**

| entry          | percent template | cycle number | time (h) | percent yield (% ee) <sup>b</sup> epoxide | percent yield (% ee) <sup>b</sup> diol |
|----------------|------------------|--------------|----------|---|--|
| 1 <sup>c</sup> | 5                | 1            | 24       | 62 (6)                                    | 6 (74)                                 |
| 2 <sup>c</sup> | 25               | 1            | 24       | 61 (13)                                   | 13 (76)                                |
| 3              | 50               | 1            | 24       | 62 (22)                                   | 20 (83)                                |
| 4 <sup>c</sup> | 50               | 1            | 48       | 66 (22)                                   | 21 (81)                                |
| 5              | 50               | 1            | 12       | 83 (3)                                    | 4 (74)                                 |
| 6              | 50               | 2            | 24       | 46 (39)                                   | 32 (85)                                |
| 7              | 50               | 3            | 24       | 50 (42)                                   | 31 (86)                                |

<sup>a</sup> Reactions run at room temperature in neat propylene oxide with water (0.55 equiv) and polymer (0.002 equiv of Co sites). <sup>b</sup> % ee determined by chiral GC analysis; the (*R*)-epoxide and the (*S*)-diol are the major enantiomers. <sup>c</sup> Average results.

supported by the loss of the Co<sup>II</sup> EPR signal and changes in the XANES spectrum to that of Co<sup>III</sup> complexes.<sup>6</sup>

The catalytic function of the materials formulated as P-1\*(py)[Co(OAc)] was tested in the HKR of propylene oxide (Table 1).<sup>6</sup> The observed trend shows a correlation between the activity toward the HKR of propylene oxide and the concentration of the template used to prepare the materials. For instance, materials prepared from 50 mol % template exhibit the highest degree of catalytic activity, yielding 62% (22% ee) epoxide and 20% (83% ee) diol (entries 1–3). The low activity observed in the materials prepared from 5 mol % template is because of the high degree of site isolation for individual cobalt complexes,<sup>5</sup> which prevents the needed interactions between metal complexes for catalysis.<sup>26,27</sup>

Entries 3, 6, and 7 in Table 1 show that the activity and selectivity of materials prepared from 50 mol % template are maintained during polymer recycling. The material activity is enhanced in subsequent cycles compared to the first (entry 3) with a 46% (39% ee) yield of epoxide and a 32% (85% ee) yield of diol achieved in cycle 2 (entry 6). We have attributed these observations to the inefficient

removal of dmap during the initial reduction step; its continued presence within the sites during the first cycle would block exogenous species access to the sites (i.e., substrate). Support for the role of dmap comes from elemental analyses that show the nitrogen content obtained for P-1\*(py)[Co<sup>III</sup>(dmap)] and P-1\*(py)[Co<sup>II</sup>] are the same. In subsequent cycles, a loss in the nitrogen content within the material is observed, which is attributed to the loss of dmap.

## Summary and Concluding Remarks

This Account described progress made in utilizing template copolymerization to prepare metal complexes within porous hosts. Our studies establish that this method can be used to design and synthesize immobilized sites with control of the primary and secondary coordination spheres of a metal. This has proven useful in tuning the functional properties of the porous materials and illustrates the importance of the immobilized site structure in maintaining function. An advantage of this approach is the use of metal-based molecular precursors as templates. Modifications to a substitutionally inert template complex led to materials with different functional properties. As shown, materials containing Co<sup>II</sup> complexes with five potential endogenous ligands function in reversible dioxygen binding, while similar materials containing only four-coordinate Co<sup>II</sup> complexes display higher affinity for NO. Site isolation within these materials prevents unfavorable bimolecular pathways that inhibit reversible binding of NO and O<sub>2</sub> in solution, thus yielding materials with different functional properties of the immobilized metal complexes compared to the corresponding monomers.

The importance of the immobilization process in regulating function was also established in development of heterogeneous catalysts. Variation of the template/



cross-linker ratio during the copolymerization process led to a series of materials displaying variable catalytic activity in the HKR of epoxides, a reaction proposed to proceed through a bimolecular pathway.<sup>26,27</sup> The activity of the material increased as the concentration of the template used to prepare the material increased. Product yields and enantioselectivities for these heterogeneous catalysts are lower than reported for related homogeneous analogues;<sup>26</sup> nevertheless, our results illustrate the promise of this approach for the development of heterogeneous catalysts.

Our findings highlight that immobilized ligands are not rigidly fixed in position, which we postulate is a consequence of the type and number of tethers that link the template to the polymeric host. In our system, this relative flexibility of immobilized groups does not appear to affect the overall function of the materials; however, function may be diminished when a more defined structure is required, such as in recognition of analytes. Moreover, the organizations of ligands within the immobilized sites are solvent-dependent, further conveying the importance of the synthetic conditions on the immobilized site formation during the copolymerization process. Additional studies are clearly needed on the structures of the immobilized sites to extend the range of functions by materials prepared by this methodology.

Support for this Account came from the PRF, ONR, DuPont, and NIH. We have worked with an outstanding group of researchers, including J. Krebs, A. Sharma, K. Padden, J. Mitchell-Koch, T. Reed, V. Joshi, S. Sharma, and R. Scarrow. We are most grateful for their efforts on this Account.

## References

- (1) Borovik, A. S. Bioinspired Hydrogen Bond Motifs in Ligand Design: The Role of Noncovalent Interactions in Metal Ion Mediated Activation of Dioxygen. *Acc. Chem. Res.* **2005**, *38*, 54–61.
- (2) Reviews: (a) Wulff, G. Molecular Imprinting in Cross-Linked Materials with the Aid of Molecular Templates—A Way towards Artificial Antibodies. *Angew. Chem., Int. Ed. Engl.* **1995**, *34*, 1812–1832. (b) *Molecular and Ionic Recognition with Imprinted Polymers*; ACS Symposium Series number 703; Bartsch, R.; Maeda, M., Eds; American Chemical Society: Washington, DC, 1998. (c) *Molecular Imprinted Polymers: Man-Made Mimics of Antibodies and Their Applications in Analytical Chemistry*; Sellergren, B., Ed.; Elsevier: Amsterdam, The Netherlands, 2001. (d) *Molecular Imprinted Materials: Science and Technology* Yan, M.; Ranström, O., Eds.; Marcel Dekker: New York, 2005.
- (3) Representative examples: (a) Dhal, P. K.; Arnold, F. H. Metal-Coordination Interactions in the Template-Mediated Synthesis of Substrate-Selective Polymers: Recognition of Bis(imidazole) Substrates by Copper(II) Iminodiacetate Containing Polymers. *Macromolecules* **1992**, *25*, 7051–7069. (b) De, B. B.; Lohray, B. B.; Sivaram, S.; Dhal, P. K. Synthesis of Catalytically Active Polymer-Bound Transition Metal Complexes for Selective Epoxidation of Olefins. *Macromolecules* **1994**, *27*, 1291–1297. (c) Santora, B. P.; Larsen, A. O.; Gagné, M. R. Toward the Molecular Imprinting of Titanium Lewis Acids: Demonstration of Diels–Alder Catalysis. *Organometallics* **1998**, *17*, 3138–3140. (d) Saunders, G. D.; Foxon, S. P.; Walton, P. H.; Joyce, M. J.; Port, S. N. A Selective Uranium Extraction Agent Prepared by Polymer Imprinting. *Chem. Commun.* **2000**, 273–274. (e) Brunkan, N. M.; Gagné, M. R. Effect of Chiral Cavities Associated with Molecularly Imprinted Platinum Centers on the Selectivity of Ligand-Exchange Reactions at Platinum. *J. Am. Chem. Soc.* **2000**, *122*, 6217–6225.
- (4) For an excellent review on the use of metal complexes in templated copolymerization, see Conrad, P. G., III; Shea, K. J. The Use of Metal Coordination for Controlling the Microenvironments of Imprinted Polymers. In *Molecular Imprinted Materials: Science and Technology*; Yan, M.; Ranström, O., Eds.; Marcel Dekker: New York, 2005, pp 123–180 and references therein.

- (5) (a) Krebs, J. F.; Borovik, A. S. Dioxygen Binding to Immobilized Co<sup>II</sup> Complexes in Porous Organic Hosts: Evidence for Site Isolation. *Chem. Commun.* **1998**, 553–554. (b) Sharma, A. C.; Borovik, A. S. Design, Synthesis, and Characterization of Templated Metal Sites in Porous Organic Hosts: Application to Reversible Dioxygen Binding. *J. Am. Chem. Soc.* **2000**, *122*, 8946–8955. (c) Padden, K. M.; Krebs, J. F.; MacBeth, C. E.; Scarrow, R. C.; Borovik, A. S. Immobilized Metal Complexes in Porous Organic Hosts: Development of a Material for the Selective and Reversible Binding of Nitric Oxide. *J. Am. Chem. Soc.* **2001**, *123*, 1072–1079. (d) Mitchell-Koch, J. T.; Reed, T. M.; Borovik, A. S. Light-Activated Transfer of Nitric Oxide from a Porous Material. *Angew. Chem. Int. Ed.* **2004**, *43*, 2806–2809.
- (6) Welbes, L. L.; Scarrow, R. C.; Borovik, A. S. Development of Porous Materials for Heterogeneous Catalysis: Kinetic Resolution of Epoxides. *Chem. Commun.* **2004**, 2544–2545.
- (7) (a) Collman, J. P.; Reed, C. A. Syntheses of Ferrous-Porphyrin Complexes. A Hypothetical Model for Deoxymyoglobin. *J. Am. Chem. Soc.* **1973**, *95*, 2048–2049. (b) Leal, O.; Anderson, D. L.; Bowman, R. G.; Basolo, F.; Burwell Jr., R. L. Reversible Adsorption of Oxygen on Silica Gel Modified by Imidazole-Attached Iron Tetraphenylporphyrin. *J. Am. Chem. Soc.* **1975**, *97*, 5125–5129.
- (8) (a) Han, H.; Janda, K. D. Soluble Polymer-Bound Ligand-Accelerated Catalysis: Asymmetric Dihydroxylation. *J. Am. Chem. Soc.* **1996**, *118*, 7632–7633. (b) Petri, A.; Pini, D.; Rapaccini, S.; Salvadori, P. Synthesis of Optically Active Diols Using an Efficient Polymer Bound Cinchona Alkaloid Derivative. *Chirality* **1995**, *7*, 580–585.
- (9) (a) Maier, W. F.; Marten, J. A.; Klein, S.; Heilmann, J.; Parton, R.; Vercruyse, K.; Jacobs, P. A. Shape-Selective Catalysis with Microporous Amorphous Mixed Oxides. *Angew. Chem., Int. Ed. Engl.* **1996**, *35*, 180–182. (b) Howe, R. F.; Lunsford, J. H. Electron Paramagnetic Resonance Studies of Some Cobalt Amine Oxygen Adducts in Zeolite Y. *J. Am. Chem. Soc.* **1975**, *97*, 5156–5159. (c) Herron, N. A. Cobalt Oxygen Carrier in Zeolite Y. A Molecular “Ship in a Bottle”. *Inorg. Chem.* **1986**, *25*, 4714–4717.
- (10) Wan, K. T.; Davis, M. E. Design and synthesis of a heterogeneous asymmetric catalyst. *Nature* **1994**, *370*, 449–450.
- (11) Lehn, J.-M. Supramolecular Chemistry—Scope and Perspectives: Molecules, Supermolecules, and Molecular Devices. *Angew. Chem., Int. Ed. Engl.* **1988**, *27*, 89–112 and references therein.
- (12) Yaghi, O. M.; Li, H.; Davis, C.; Richardson, D.; Groy, T. L. Synthetic Strategies, Structure Patterns, and Emerging Properties in the Chemistry of Modular Porous Solids. *Acc. Chem. Res.* **1998**, *31*, 474–484 and references therein.
- (13) Sokol, J. J.; Hee, A. G.; Long, J. R. A Cyano-Bridged Single-Molecule Magnet: Slow Magnetic Relaxation in a Trigonal Prismatic MnMo<sub>6</sub>(CN)<sub>18</sub> Cluster. *J. Am. Chem. Soc.* **2002**, *124*, 7656–7657.
- (14) Beil, J. B.; Zimmerman, S. C. A Monomolecularly Imprinted Dendrimer (MID) Capable of Selective Binding with a Tris(2-aminoethyl)amine Guest through Multiple Functional Group Interactions. *Chem. Commun.* **2004**, 488–489.
- (15) For an example on the analysis of small-molecule binding using spectroscopic techniques, see Shea, K. J.; Sasaki, D. Y. An Analysis of Small-Molecule Binding to Functionalized Synthetic Polymers by <sup>13</sup>C CP/MAS NMR and FT-IR Spectroscopy. *J. Am. Chem. Soc.* **1991**, *113*, 4109–4120.
- (16) (a) Shea, K. J.; Thompson, E. A. Template Synthesis of Macromolecules. Selective Functionalization of an Organic Polymer. *J. Org. Chem.* **1978**, *43*, 3, 4253–4255. (b) Shea, K. J.; Thompson, E. A.; Pandey, S. D.; Beauchamp, P. S. Template Synthesis of Macromolecules. Synthesis and Chemistry of Functionalized Macroporous Polydivinylbenzene. *J. Am. Chem. Soc.* **1980**, *102*, 3149–3155. (c) Damen, J.; Neckers, D. C. Stereoselective Syntheses via a Photochemical Template Effect. *J. Am. Chem. Soc.* **1980**, *102*, 3265–3267.
- (17) Padden, K. M.; Krebs, J. F.; Trafford, K. T.; Yap, G. P. A.; Rheingold, A. H.; Borovik, A. S.; Scarrow, R. C. Probing the Structure of Immobilized Metal Sites in Porous Organic Hosts by X-ray Absorption Spectroscopy. *Chem. Mater.* **2001**, *13*, 4305–4313.
- (18) Cesarotti, E.; Gullotti, M.; Pasini, A.; Ugo, R. Optically Active Complexes of Schiff Bases. Part 5. An Investigation of Some Solvent and Conformational Effects on the Equilibria between Cobalt(II) Schiff-Base Complexes and Dioxygen. *J. Chem. Soc., Dalton Trans.* **1977**, 757–763.
- (19) Allender, C. J.; Heard, C. M.; Brain, K. R. Mobile Phase Effects on Enantiomer Resolution Using Molecularly Imprinted Polymers. *Chirality* **1997**, *9*, 238–242 and references therein.
- (20) Jones, R. D.; Summerville, D. A.; Basolo, F. Synthetic Oxygen Carriers Related to Biological Systems. *Chem. Rev.* **1979**, *79*, 139–179.

- (21) (a) Moncada, S.; Palmer, R. M. J.; Higgs, E. A. Nitric Oxide: Physiology, Pathophysiology, and Pharmacology. *Pharmacol. Rev.* **1991**, *43*, 109–142. (b) *Nitric Oxide: Biology and Pathobiology*; Ignarro, L. J., Ed.; Academic Press: New York, 2000.
- (22) (a) Wink, D. A.; Mitchell, J. B. Chemical Biology of Nitric Oxide: Insights into Regulatory, Cytotoxic, and Cytoprotective Mechanisms of Nitric Oxide. *Free Radical Biol. Med.* **1998**, *25*, 434–456. (b) Lincoln, J.; Hoyle, C. H. V.; Burnstock, G. *Nitric Oxide in Health and Disease*; Cambridge University Press: New York, 1997.
- (23) Clarkson, S. G.; Basolo, F. Study of the Reaction of Some Cobalt Nitrosyl Complexes with Oxygen. *Inorg. Chem.* **1973**, *12*, 1528–1534.
- (24) (a) Works, C. F.; Ford, P. C. Photoreactivity of the Ruthenium Nitrosyl Complex, Ru(salen)(Cl)(NO). Solvent Effects on the Back Reaction of NO with the Lewis Acid Ru<sup>III</sup>(salen)(Cl). *J. Am. Chem. Soc.* **2000**, *122*, 7592–7593. (b) Works, C. F.; Jocher, C. J.; Bart, G. D.; Bu, X.; Ford, P. C. Photochemical Nitric Oxide Precursors: Synthesis, Photochemistry, and Ligand Substitution Kinetics of Ruthenium Salen Nitrosyl and Ruthenium Salophen Nitrosyl Complexes. *Inorg. Chem.* **2002**, *41*, 3728–3739. (c) Bordini, J.; Hughes, D. L.; da Motta Neto, J. D.; da Cunha, C. J. Nitric Oxide Photorelease from Ruthenium Salen Complexes in Aqueous and Organic Solutions. *Inorg. Chem.* **2002**, *41*, 5410–5416.
- (25) NO is rapidly converted to nitrite under the experimental conditions. Schmidt, H. H. H. W.; Kelm, M. Determination of Nitrite and Nitrate by the Griess Reaction. In *Methods in Nitric Oxide Research*; Feelisch, M., Stamler, J. S., Eds.; Wiley and Sons: New York, 1996; Chapter 33.
- (26) (a) Tokunaga, M.; Larrow, J. F.; Kakiuchi, F.; Jacobsen, E. N. Asymmetric Catalysis with Water: Efficient Kinetic Resolution of Terminal Epoxides by Means of Catalytic Hydrolysis. *Science* **1997**, *277*, 936–938. (b) Schaus, S. E.; Brandes, B. D.; Larrow, J. F.; Tokunaga, M.; Hansen, K. B.; Gould, A. E.; Furrow, M. E.; Jacobsen, E. N. Highly Selective Hydrolytic Kinetic Resolution of Terminal Epoxides Catalyzed by Chiral (salen)Co<sup>III</sup> Complexes. Practical Synthesis of Enantioenriched Terminal Epoxides and 1,2-Diols. *J. Am. Chem. Soc.* **2002**, *124*, 1307–1315 and references therein.
- (27) Nielsen, L. P. C.; Stevenson, C. P.; Blackmond, D. G.; Jacobsen, E. N. Mechanistic Investigation Leads to a Synthetic Improvement in the Hydrolytic Kinetic Resolution of Terminal Epoxides. *J. Am. Chem. Soc.* **2004**, *126*, 1360–1362 and references therein.
- (28) Walker, F. A. An Electron Spin Resonance Study of Coordination to the Fifth and Sixth Positions of  $\alpha,\beta,\gamma,\delta$ -Tetra(*p*-methoxyphenyl)-prophinatecobalt(II). *J. Am. Chem. Soc.* **1970**, *92*, 4235–4244.

AR0402513